Pervaporation Properties of Aromatic/Nonaromatic Hydrocarbons of Crosslinked Membranes of Copolymers Based on Diethyl Vinylbenzylphosphonate

Yong Wang, Satoshi Hirakawa, Kazuhiro Tanaka, Hidetoshi Kita, Ken-ichi Okamoto

Department of Advanced Materials Science and Engineering, Faculty of Engineering, Yamaguchi University, Ube, Yamaguchi 755-8611, Japan

Received 29 October 2001; accepted 17 April 2002

ABSTRACT: Copoly(diethyl vinylbenzylphosphonate/hydroxyethyl methacrylate) [copoly(VBP–HEMA)] and copoly(diethyl vinylbenzylphosphonate/vinylbenzyl chloride) [copoly(VBP–VBC)] were prepared and their membranes crosslinked by a reaction of ethylene glycol diglycidyl ether and ethylene diamine with, respectively, hydroxyl and methylene chloride groups in their side chains. Pervaporation (PV) and sorption of benzene–*n*-hexane (Bz–Hx), benzene–cyclohexane (Bz–Cx), and toluene–*n*-octane (Tol–*n*-Ot) mixtures were investigated. The membranes were in a rubbery state and preferentially permeable to aromatics. They had higher specific permeation flux and a lower PV separation factor compared with the crosslinked membranes of methacrylate copolymers with analogous pendant groups. They displayed better PV performance for Tol–*n*-Ot. Sorption isotherms of Bz–Hx mixtures were represented by the Flory–Rehner model. © 2003 Wiley Periodicals, Inc. J Appl Polym Sci 87: 2177–2185, 2003

Key words: pervaporation; sorption; diffusion; hydrocarbons separation; membrane

INTRODUCTION

Pervaporation (PV) has attracted much attention for separation of azeotropic or close-boiling liquid mixtures with reduced energy consumption. The separation of aromatics from hydrocarbon mixtures is one of the separation processes in petroleum refining in which membrane separation may have a significant impact. Many polymer membranes have been studied for PV of aromatic/nonaromatic hydrocarbon mixtures.[1–21]

PV in polymer membranes is described by a solution–diffusion mechanism and separation by a solubility selectivity and diffusivity mechanism. For PV of aromatic/alicyclic and aromatic/branched-aliphatic hydrocarbons such as Bz–Cx and toluene–isooctane (Tol–i-Ot), glassy polymer membranes such as sulfonyl-containing polyimides have relatively high performance with high selectivity in compensation for low permeability.[10,14] The high selectivity is a result of a combination of the relatively high solubility and diffusivity selectivity. On the other hand, these glassy polymer membranes have rather poor performance with not-so-high selectivity and low permeability for PV of aromatic/*n*-aliphatic hydrocarbons such as benzene–*n*-hexane (Bz–Hx) and toluene/*n*-octane (Tol–*n*-Ot). This is because of loss of the diffusivity selectivity. These are attributed to the dense packing of rigid polymer chains and the difference in the molecular size of penetrants.

Compared with glassy polymers, rubbery polymers generally have higher permeability because of a higher free-volume fraction and flexible polymer chains.[8,9,13] Therefore, to achieve both high selectivity and high permeability, rubbery polymers designed to have high affinity to aromatics and simultaneously to suppress excessive membrane swelling seem a better candidate than glassy polymers for being excellent PV membrane material. Typical examples of such membranes are hard-/soft-segmented copolymer membranes[8,9,13] and graft-filling polymerized membranes,[4,5,12,20] in which the rubbery polymers govern both selectivity and permeability and the polyimide hard segments or the porous inert substrate contributes to suppression of excessive membrane swelling.

Among the polymers investigated so far, excellent performance for PV of Bz–Cx has been reported for the crosslinked membranes of polymer alloys of poly(styrene diethyl phosphonate) and cellulose acetate (CA) [P-PS/CA],[1,2] of poly(phenylene oxide diethyl phosphonate) with CA (P-PPO/CA),[11] and of polyimides with pendant phosphonate ester groups (P-PI).[11]

Correspondence to: K. Okamoto (okamotok@po.cc.yamaguchi-u.ac.jp).

Contract grant sponsor: Ministry of Education, Culture, Sports, Science, and Technology of Japan Grand-in-Aid for Developmental Scientific Research; contract grant number: 10450296.

Contract grant sponsor: Petroleum Energy Center and Japan Chemical Innovation Institute.

Journal of Applied Polymer Science, Vol. 87, 2177–2185 (2003)

The high performance of these membranes has been attributed mainly to the high affinity of the phosphonate ester groups to Bz. These membranes were in a glassy state. It is interesting to investigate the PV properties of aromatic/*n*-aliphatic hydrocarbon mixtures of crosslinked membranes of rubbery polymers with pendant phosphonate or analogous groups.

In a previous article we reported on the PV properties of crosslinked membranes of copoly(methacrylate) with pendant phosphate and/or carbamoylphosphonate groups.[21] Some of them displayed higher PV performance to the Bz–Hx and Tol–*n*-Ot systems. They displayed higher separation factors and lower specific permeation fluxes than those of poly(ethylene oxide imide)–segmented block copolymer (PEO-PI) membranes. The higher selectivity was a result of both reasonably high solubility selectivity and a small but positive contribution of diffusivity selectivity. The lower permeability resulted from lower diffusivity. Although in a rubbery state, these membranes displayed characteristics of glassy polymers rather than those of rubbery ones, probably because of dense polymer-chain packing from the hydrogen bonding between carbonyl and hydroxyl groups of the polymer side chains. The present article takes up the PV of Bz–Hx, Bz–Cx, and Tol–*n*-Ot through crosslinked membranes of copolymers based on diethyl vinylbenzylphosphonate (VBP).

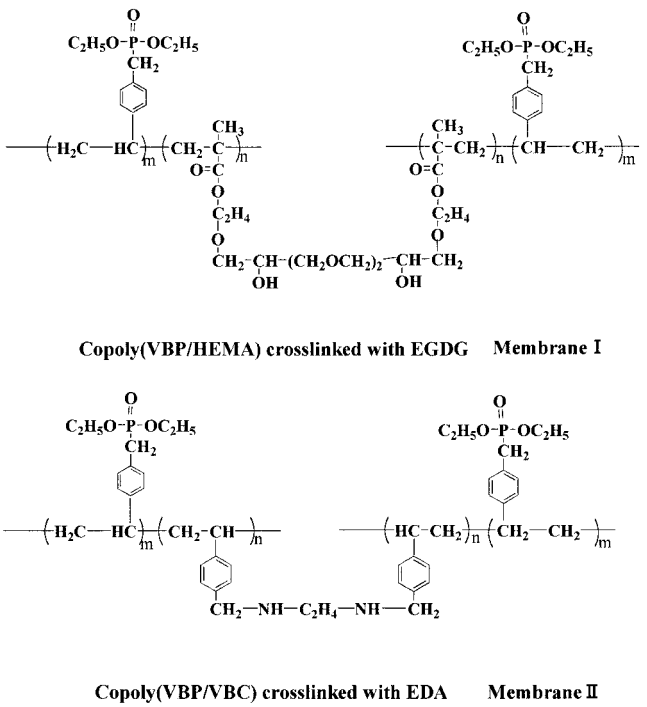

Figure 1 Chemical structures of crosslinked membranes of styrene copolymers with pendant phosphonate group.

EXPERIMENTAL

Membrane preparation

Hydroxyethyl methacrylate (HEMA) and vinylbenzyl chloride (VBC) were purified by vacuum distillation. VBP was prepared according to the literature.[22]

A THF solution (20 cm^3) containing 15 wt % monomers and 0.5 wt % azobisisobutyronitrile to monomer was poured into a Pyrex glass tube and degassed three times in freeze–thaw cycles. Polymerization was carried out in the sealed tube at 343 K for 48 h, and then the solution was poured into excessive Hx. The copolymer was purified by reprecipitation from THF–Hx and dried at 333 K *in vacuo* for 8 h. The yields were more than 90% for copoly(VBP–HEMA), and 70%–80% for copoly(VBP–VBC). The monomer molar ratio in copoly(VBP–HEMA) was considered the same as that in feed because of the almost 100% yield. The molar ratio in copoly(VBP–VBC) was determined from the integral intensity ratio of the signal of phenyl protons (6.2–7.2 ppm) over the signal of chloromethylene protons (4.4–4.6 ppm) in the ^{1}H-NMR spectra.

Ethylene glycol diglycidyl ether (EGDE) or ethylene diamine (EDA) was used as a crosslinking reagent, of which the molar number was half that of HEMA or VBC in the copolymer. Membranes were cast from the THF solution of the copolymer and the crosslinking reagent onto Teflon Petri dishes, and then dried at room temperature for 8 h and at 313 K for 4 h for copoly(VBP–HEMA) or at 353 K for 8 h for copoly(VBP–VBC) in an air oven. The copoly(VBP–HEMA) membranes were further heat-treated at 423 K for 6 h *in vacuo* for the crosslinking reaction of —CH_2OH with epoxy groups. The chemical structures of the crosslinked copolymer membranes are shown in Figure 1.

Measurements

Differential scanning calorimetry (DSC) was done with a Seiko Instruments, Inc., DSC-5200 (Japan) at a heating and cooling rate of 10 K/min. The glass-transition temperature, T_g, was determined from the onset points of the signals on the first heating run. The ^{1}H-NMR spectra were recorded on a JEOL 270 MHz spectrometer using chloroform-d_1 as solvent.

PV experiments were carried out by an ordinary method. The effective membrane area was about 22 cm^2, and the volume of feed solution was about 100 mL. The pressure at the downstream side was maintained below 0.2 torr. The permeate was collected by a cold trap in liquid nitrogen. Feed and permeate composition was analyzed by gas chromatography. The separation factor of PV, α_{PV}, is defined by eq. (1):

$$\alpha_{PV} = y(1 - x)/x(1 - y) \quad (1)$$

where x and y are weight fractions (%) of aromatic components in feed and permeate, respectively.

Transient sorption and desorption experiments were carried out at 333 K and at vapor activities up to 0.85, using a sorption apparatus equipped with either a quartz spring or a Sartorius electronic microbalance. The weight of membrane samples used was 70–100 mg. Plots of M_t/M_∞ versus $t,^{1/2}$ where M_t and M_∞ refer to the mass sorbed (or desorbed) at time t and at infinite (or zero) time, respectively, initially were linear. Diffusion coefficients for sorption and desorption (D_s and D_d, respectively) were determined from the initial slopes according to eq. (2)[23]:

$$M_t/M_\infty = 4\ (Dt/\pi\ l^2)^{1/2} \tag{2}$$

The diffusion coefficient, D, used in this study was calculated as the average of D_s and D_d. The sorption amount S was defined as

$$S = 100(W_s - W_d)/W_d \tag{3}$$

where W_d and W_s are the weights of dry and solvent-swollen membranes, respectively.

Single-component liquid sorption was also measured by immersing the membrane pieces (0.1–0.2 g) in a solvent. The membrane pieces were taken out, wiped with tissue paper, and weighed on a microbalance. For binary component sorption, membrane pieces of 10–30 mg were immersed in Bz–Hx mixtures at 333 K for 3–5 h. The membrane pieces were wiped quickly with tissue paper and put in vial glass tubes. The sorbed amounts of each component were measured by the multiple headspace extraction method using a headspacer sampler HS-40 (Perkin Elmer) and a capillary gas chromatograph GC-17A (Shimadzu) equipped with DB-WAX-30N-STD. The data in this article are average values of 4–5 measurements. The solubility selectivity, α_s, was calculated using eq. (1) as in the PV by redefining x and y as weight fractions of the Bz component in the solvent mixture and membrane, respectively.

The concentration-averaged diffusion coefficient of component i, $\bar{D}_i$, was calculated from eq. (4),

$$\bar{D}_i = q_i l/C_i \tag{4}$$

where q_i is permeation flux of component i, l is membrane thickness, and C_i is the concentration of component i in the membrane at the feed side, which was calculated from the sorption amount of the component, assuming the additivity of membrane density.

Diffusivity selectivity α_D was calculated from eq. (5):

$$\alpha_D = \alpha_{PV}/\alpha_S \tag{5}$$

RESULTS AND DISCUSSION

Characterization of crosslinked membranes

Characterization results of the crosslinked membranes are summarized in Table I. The membranes were crosslinked by the reaction of —OH or —CH_2Cl groups with epoxy or amine groups at 423 K and 353 K, respectively. After the crosslinking the membranes became insoluble in any solvents. The crosslinked copolymer membranes had glass-transition temperatures below 310 K and were in rubbery state at the measurement temperatures of PV and sorption. With an increase in molar ratio of VBP in the copolymers, the crosslinking degree decreased and the phosphorous content increased a little. The densities of the membranes were in the range of 1.18–1.20 g/cm^3, which were lower than those (1.25–1.28 g/cm^3) of the crosslinked membranes of copoly(methacrylate) with pendant phosphate and carbamoylphosphonate groups, namely, copoly(DEMP–HEMA) and copoly(DEMP–DEMCP), where DEMP and DEMCP refer to diethyl 2-methacryloyloxyethyl phosphate and diethyl *N*-[2-(methacryloyloxy)ethyl] carbamoylphosphonate, respectively.[21] The solubility parameter δ values of the membranes, which were calculated by the group contribution method,[24] were in the range of 19.8–20.2 (J/cm^3)$^{1/2}$ and a little lower than those of the copoly(methacrylate) membranes.

TABLE I
Characterization of Crosslinked Membranes of Copoly(VBP/HEMA) and Copoly(VBP/VBC)

Polymer code No.	Molar ratio[a]	*P* content (wt %)	Density (g/cm^3)	Tg (K)	δ (J/cm^3)$^{1/2}$
Copoly(VBP/HEMA) crosslinked with EGDE					
I-1	5:1	10.7	1.18	309	20.2
I-2	7:1	11.0	1.19	295	20.0
Copoly(VBP/VBC) crosslinked with DEA					
II-1	5.6:1	10.7	1.20	299	20.0
II-2	10.9:1	11.2	1.20	286	19.8

[a] Molar ratio of VBP over HEMA or VBC.

PV properties of crosslinked membranes

The physical properties of penetrant molecules are listed in Table II. In Bz–Hx, Bz–Cx, and Tol–*n*-Ot systems, the specific permeation flux, Ql, and the separation factor, α_{PV} at a feed composition of Bz and Tol (x_{Bz} and x_{Tol}) of 20 wt % are listed in Table III. Figure 2(a–c) shows plots of the specific permeation flux of each component ql and α_{PV} versus feed composition for these systems. The membranes were preferentially permeable to Bz or Tol over Cx, Hx, or *n*-Ot. They displayed a little higher PV performance (a little larger Ql and α_{PV}) for the Bz–Cx system than for the Bz–Hx. On the other hand, they displayed smaller Ql and higher α_{PV} values for the Tol–*n*-Ot system than for the other two systems.

With an increase in molar ratio of VBP, Ql increased a little and α_{PV} decreased a little because of an increase in membrane swelling as a result of the reduced degree of crosslinking. Compared with membrane II-1,

TABLE II
Physical Properties of Penetrants[a]

Penetrant	σ_{LJ} (nm)	a_D (nm^2)	δ (J/cm^3)$^{1/2}$
Benzene (Bz)	0.527	0.21	18.5
Toluene (Tol)	0.593	0.23	18.2
n-Hexane (Hx)	0.591	0.18	14.9
Cyclohexane (Cx)	0.609	0.33	16.7
n-Octane (*n*-Ot)	0.745	0.18	14.9
iso-Octane (i-Ot)	0.762	0.36	14.1

σ_{LJ} is Lennard–Jones collision diameter[25]; δ is solubility parameter; a_D is diffusional cross-section area and determined as the product of the smallest and the next smallest dimensions measured by using a Stuard-type molecular model (CPK model).

which has a molar ratio (5–5.6) similar to VBP, membrane I-1 displayed a larger Ql and a little smaller α_{PV}, probably because of the much softer crosslinking linkage.

As shown in Figure 2(a,b), these membranes showed a similar feed composition dependence of ql and α_{PV} between the Bz–Hx and Bz–Cx systems. With an increase in x_{Bz}, $q_{Bz}l$ increased significantly, and both $q_{Hx}l$ and $q_{Cx}l$ also increased in the range of x_{Bz} of less than 50 wt %. As a result, with an increase in x_{Bz}, α_{PV} decreased significantly. This feed composition dependence is characteristic of rubbery polymeric membranes such as PEO-PI[13] and copoly(DEMP–HEMA) and copoly(DEMP–DEMCP).[21] This appears to be a result of increases in diffusivity and solubility with an increase in x_{Bz} because of increasing membrane swelling.[13] This feed composition dependence is larger for the present membranes than for the other membranes reported. As shown in Figure 2(c), a similar characteristic was also observed for the Tol–*n*-Ot system.

Figure 3(a–c) shows the temperature dependence of ql and α_{PV}. The activation energies of permeation flux were about 50 kJ/mol for Bz and 60–65 kJ/mol for Hx and Cx at an x_{Bz} of 20 wt % in the Bz–Hx and Bz–Cx systems. They were about 45 and 60 kJ/mol for Tol and *n*-Ot, respectively, at an x_{Tol} of 40 wt % in the Tol–*n*-Ot system. These values were a little lower than those of crosslinked membranes of methacrylate copolymers with pendant phosphate and carbamoylphosphonate groups[21] and were higher than those of PEO-PI membranes.[13]

Sorption and diffusion properties of crosslinked membranes

Vapor sorption of single component Bz and Hx was measured for membrane II-1 at 333 K. The sorption and desorption behavior of vapors was classified as the normal Fickian diffusion. Vapor activity dependence of diffusion coefficient D determined from Eq. (2) is shown in Figure 4. With an increase in vapor activity, D_{Bz} increased significantly, but D_{Hx} hardly increased. This is because of the significant difference in the sorption amounts between Bz and Hx, namely, the difference in membrane swelling. The diffusion coefficient extrapolated to the activity of zero, D_o, was similar that between Bz and Hx.

Sorption isotherms of Bz and Hx vapors in membrane II-1 are shown in Figure 5. For binary system (one solvent and one polymer), Flory-Rehner model is often used for the description of sorption equilibrium of a crosslinked polymeric film.[26,27]

$$\ln(a) = \ln(\phi_1) + (1 - \phi_1) + \chi_{1p}(1 - \phi_1)^2 + KV_1(1 - \phi_1)\{I - (1 - \phi_1)^{1/3}\} \quad (6)$$

where a is activity, ϕ_1 is the volume fraction of solvent, χ_{1p} is the polymer–solvent interaction parameter; K is a characteristic constant of the polymer, and V_1 is molar volume of the solvent. In the present study, χ_{1p} and K were used as adjustable parameters in order to obtain the best fit of the model to the experimental data. The best-fit parameters were $K = 0.10$ and $\chi_{1p} = 0.680$ (Bz) and 2.35 (Hx). The solid lines in Figure 5 represent the sorption isotherms calculated using these parameter values. Compared with crosslinked membranes of copoly(DEMP–HEMA),[21] membrane II-1 had a smaller χ_{1p} value of Bz, indicating a higher affinity to Bz.

Sorption of binary Bz–Hx liquid mixtures was measured for membrane II-1 at 333 K. The sorption amounts for each component, S_{Bz} and S_{Hx}, are plotted against x_{Bz} in Figure 6.

It is possible to readily extend eq. (6) to a ternary system (two solvents and one polymer),

$$\ln(a_1) = \ln(\phi_1) + (1 - \phi_1) - \phi_2\left(\frac{V_1}{V_2}\right) + (\chi_{12}\phi_2 + \chi_{13}\phi_3) \times (\phi_2 + \phi_3) - \chi_{23}\left(\frac{V_1}{V_2}\right)\phi_2\phi_3 + KV_1\phi_3(1 - \phi_3^{1/3})$$

TABLE III
PV Properties of Crosslinked Copolymer Membranes Toward Bz/Hx, Bz/Cx, and Tol/*n*-Ot systems Ot 20 wt % X_{Bz} and X_{Tol}

Membrane	System	Temperature (K)	Q1 (kg μm/m^{2}h)	α_{PV}
I-1	Bz/Hx	323	2.0	12.0
I-2	″	″	2.5	11.5
II-1	″	″	0.94	13.0
II-2	″	″	1.5	12.0
I-1	Bz/Cx	333	3.6	13.0
I-2	″	″	4.3	11.9
II-1	″	″	1.8	13.7
II-2	″	″	2.6	12.4
I-2	Tol/n-Ot	323	1.1	22.1
II-1	″	333	0.39	30.6
II-2	″	″	0.80	24.5

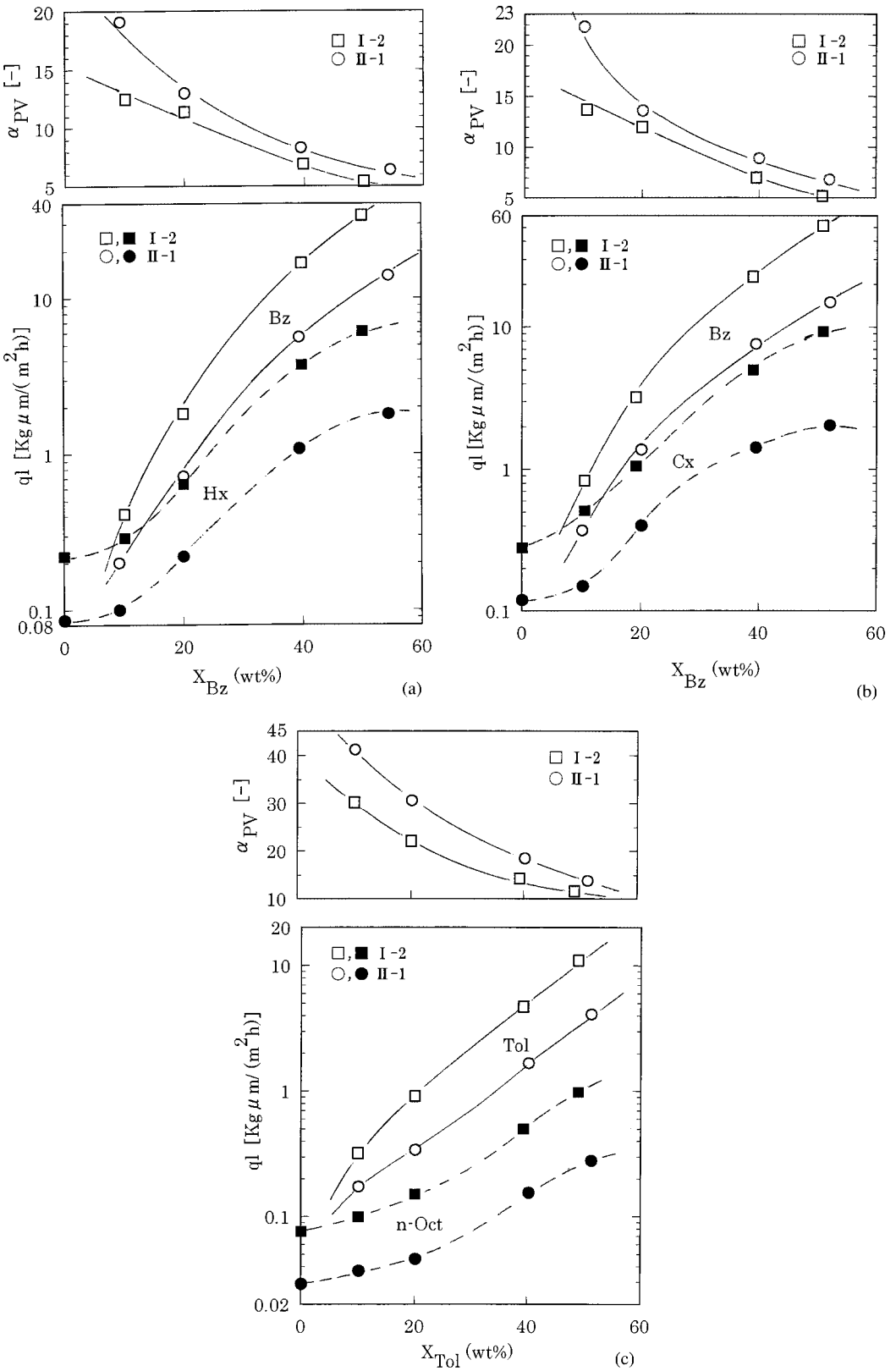

Figure 2 Feed composition dependence of separation factor and specific permeation flux of each component in crosslinked membranes I-2 and II-1 for (a) Bz–Hx, (b) Bz–Cx, and (c) Tol–*n*-Ot systems.

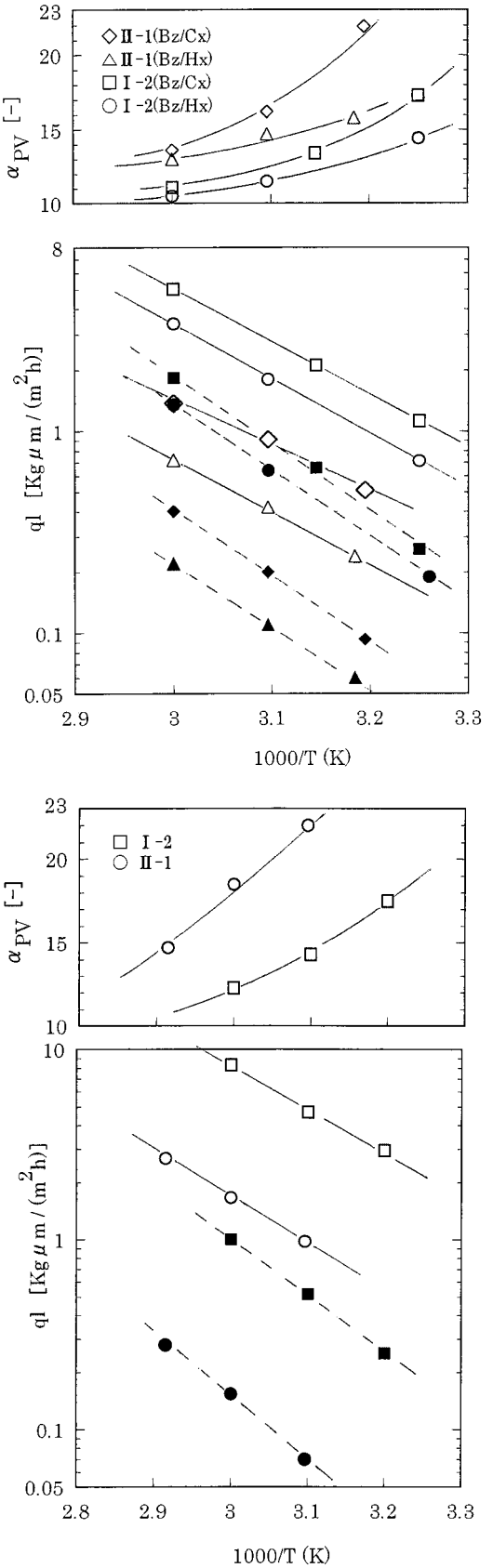

Figure 3 Temperature dependence of separation factor and specific permeation flux of each component in crosslinked membranes I-2 and II-1 for (a) Bz–Hx and Bz–Cx (x_{Bz} = 20 wt %) and (b) Tol–*n*-Ot (x_{Tol} = 40 wt %). In bottom figures, open keys are for $q_{Bz}l$ and $q_{Tol}l$, and closed keys are for $q_{Hx}l$, $q_{Cx}l$, and $q_{Bn\text{-}Ot}l$.

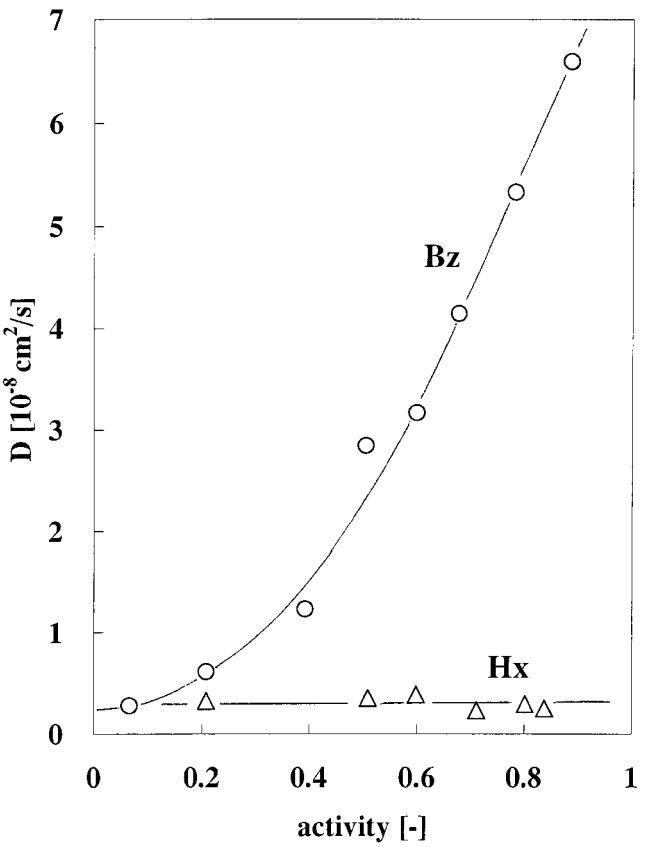

Figure 4 Activity dependence of diffusion coefficient of Bz and Hx vapors in membrane II-1 at 333 K.

$$\ln(a_2) = \ln(\phi_2) + (1 - \phi_2) - \phi_1\left(\frac{V_2}{V_1}\right) + \left\{\chi_{12}\phi_1\left(\frac{V_2}{V_1}\right) + \chi_{23}\phi_3\right\}(\phi_1 + \phi_3) - \chi_{13}\left(\frac{V_2}{V_1}\right)\phi_1\phi_3 + KV_2\phi_3(1 - \phi_3^{1/3}) \quad (7)$$

where a_i, ϕ_i, and V_i are the activity, volume fraction, and molar volume, respectively, of solvent *I;* and χ_{ij} is the interaction parameter of components *i* and *j*. The subscripts 1, 2, and 3 refer to the major sorption component (Bz), the minor component (Hx), and polymer, respectively. The χ_{12} values were determined to be 0.55 (Bz–Hx) from liquid–vapor equilibrium data. Using the Flory–Rehner sorption parameters, the ternary sorption isotherms were calculated from eq. (7), and the results are shown by solid lines in Figure 6. The calculated sorption isotherm of Bz was in agreement with the experimental one, whereas the calculated isotherm of the minor sorption component, Hx, was a little smaller than the experimental one. As a result, the solubility selectivity α values predicted by the Flory–Rehner model were a little higher than the experimental values. This was different from the Bz–Hx sorption in PEO-PI[13] and copoly(DEMP–HEMA).[21]

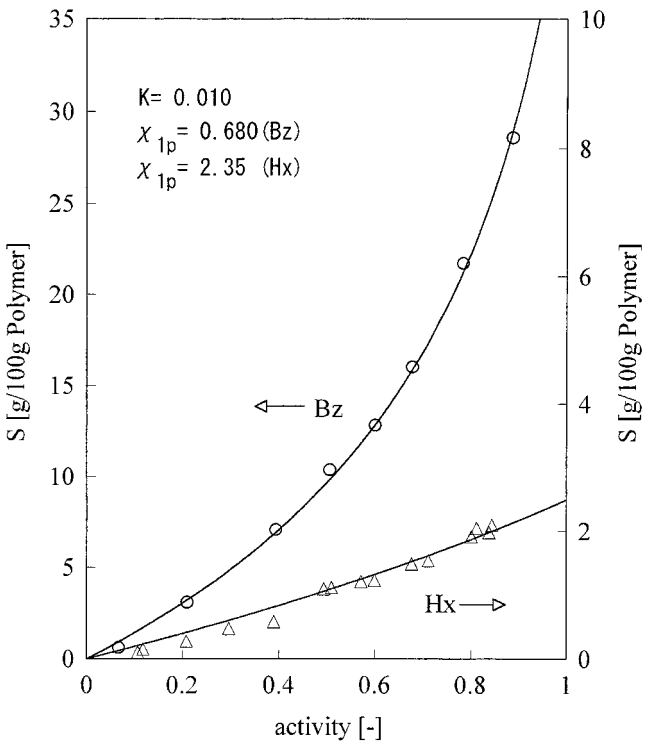

Figure 5 Sorption isotherms of Bz and Hx vapors in membrane II-1 at 333 K. The solid lines were calculated using the Flory–Rehner model.

The sorption data of membrane II-1 for Bz–Hx system are listed in Table IV. The concentration-averaged diffusion coefficients, $\bar{D}_{Bz}$ and $\bar{D}_{Hx}$, and the diffusivity selectivity, α_d, determined from eqs. (4) and (5), respectively, are listed in Table IV. For comparison the sorption, diffusion, and PV data of other polymers are also listed in Table IV.[13,21]

Compared with copoly(DEMP–HEMA) and copoly(DEMP–DEMCP),[21] membrane II-1 had a larger sorption amount and smaller solubility selectivity. The diffusion coefficients were also larger for membrane II-1. As a result, membrane II-1 displayed higher permeation flux but lower PV selectivity. The smaller sorption and lower diffusivity for the former DEMP-based membranes can be explained by dense polymer chain packing from the hydrogen bonding between the carbonyl and hydroxy groups of the polymer side chain as well as a much higher crosslinking density.[21] On the other hand, the present VBP-based membranes had a higher affinity for Bz and a lower crosslinking density and no effect or much less effect from the hydrogen bonding, resulting in larger membrane swelling in the feed and in higher diffusivity.

Compared with PEO-PI, membrane II-1 displayed a smaller sorption amount and smaller solubility selectivity, whereas they displayed much smaller diffusion coefficients and larger diffusivity selectivity. In particular, the diffusivity selectivity was positive, namely, $\alpha_D > 1$. This is quite similar to the case of copoly(DEMP–HEMA) and copoly (DEMP–DEMCP) and different from that of PEO-PI, for which diffusivity selectivity was negative, namely, $\alpha_D < 1$, for the Bz–Hx system. The much smaller specific permeation flux of membrane II-1 was attributed mainly to much smaller diffusion coefficients.

Comparison of membrane performances

Table V shows a comparison of membrane performances to PV of the Bz–Hx, Bz–Cx, and Tol–*n*-Ot systems among the present and other polymer membranes. For the PV of Bz–Hx, the crosslinked membranes of copoly(DEMP–HEMP) and copoly(DEMP–DEMCP) displayed as high a performance as the P-PI and PEO-PI membranes; these membranes form a trade-off line between α_{PV} and Ql.[21] Compared with these membranes, the present VBP-based membranes, I-2, II-1, and II-2, displayed rather poor PV performance, probably because of larger membrane swelling, as mentioned above.

For the PV of Tol–*n*-Ot, the present membranes displayed good performance, compared with the

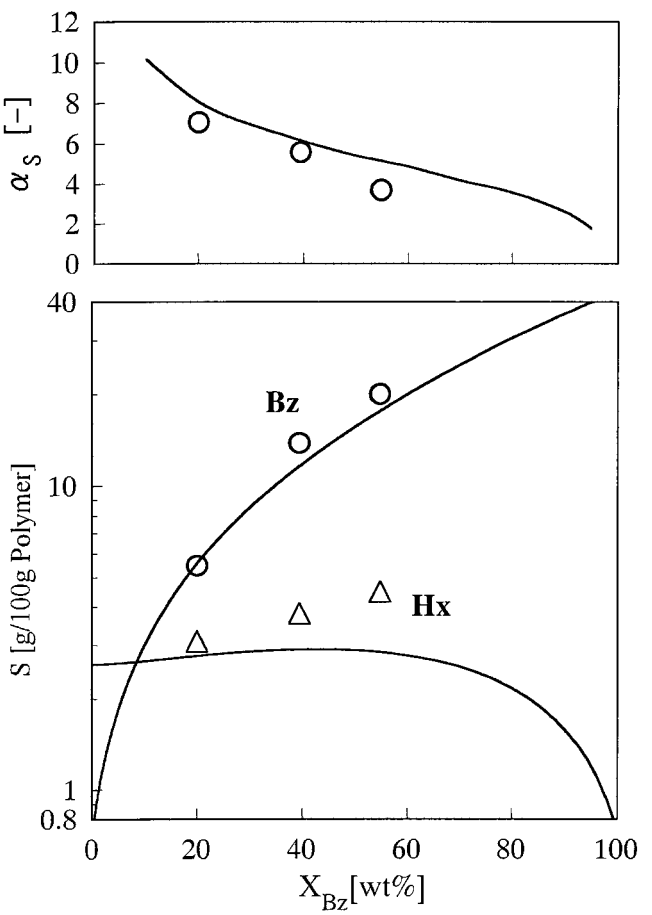

Figure 6 Feed composition dependence of solubility selectivity and sorption amount of each component for Bz–Hx mixtures in membrane II-1 at 333 K. The solid lines were calculated using the Flory–Rehner model.

TABLE IV
Sorption, Diffusion, and PV Properties of Membranes for Bz/Hx System at 333 K

Membrane No.	X_{Bz} (wt %)	S_{Bz} (g/100 g dry polymer)	S_{Hx} (g/100 g dry polymer)	α_S	α_D	α_{PV}	$q_{Bz}l$ (kg μm/(m^{2}h))	$q_{Hx}l$ (kg μm/(m^{2}h))	$\bar{D}_{Bz}$ (10^{-8} cm^2/s)	$\bar{D}_{Hx}$ (10^{-8} cm^2/s)	Ref
II-1	20	5.5	3.1	7.0	1.9	13.0	0.72	0.22	3.6	2.0	This
II-1	40	13.8	3.8	5.2	1.6	8.3	5.6	1.1	12	8.6	
II-1	54	20.0	4.5	3.7	1.7	6.4	13.9	1.8	23	13.2	
DEMP/HEMA (I-2)	50	10.0	1.3	7.5	1.3	9.4	4.3	0.48	10	9.1	21
DEMP/DEMCP(IV-3)	″	10.4	1.2	8.7	1.1	9.1	5.7	0.62	13.4	12.0	21
PEO–PI[a]	″	17.5	1.9	8.2	0.75	6.2	40	6.2	81	119	13
		(32)	(3.6)						(150)	(220)	
DSDA–DDBT	50	14.3	1.8	7.8	1.25	9.8	1.32	0.14	2.4	1.8	14
P–PI	60	16.5	1.5	7.6	1.2	8.8	6.5	0.49	11	9.2	11

[a] PEO content is 54.4 wt %. Numerals in the parentheses are for PEO segment domains, and the other numerals are for overall polymer matrix.

DEMP-based copolymer membranes, and formed a trade-off line between α_{PV} and *Ql* together with PEO-PI and P-PI. The reason for this is not clear at present. A possibility for consideration is that the membrane swelling was not as large in Tol–*n*-Ot as in Bz–Hx, and as a result the present membranes were able to maintain relatively high α_{PV} values together with high *Ql*.

For the PV of Bz–Cx, the present VBP-based membranes as well as the other rubbery polymer membranes such as the DEMP-based copolymers and PEO-PI displayed poor performance compared with the glassy polymer membranes such as P-PI, P-PS–CA, and DSDA-DDBT. The former membranes were below the trade-off line between α_{PV} and *Ql* formed by the latter membranes.

Note that the P-PI membranes, although in a glassy state under PV, displayed excellent PV performance not only to Bz–Cx but also to Bz–Hx and Tol–*n*-Ot and formed the upper-bound trade-off lines between α_{PV} and *Ql* for these three systems. This is different from the case with sulfonyl-containing polyimide membranes such as DSDA-DDBT. This might be because of the differences in diffusivity; diffusivity was much higher for P-PI than for DSDA-DDBT, and the contribution of α_D to the PV performance to Bz–Cx was much smaller.

TABLE V
Membrane performance toward PV of Bz/Hx, Bz/Cx and Tol/n-Ot systems at x_{Bz} and x_{Tol} of 40 wt%

Membranes No	System	Temp (K)	Ql (kg μm/m^{2}h)	α_{PV}	Reference
I-2	Bz/Hx	323	20.6	6.9	This article
II-1	Bz/Hx	333	6.7	8.3	This article
II-2	Bz/Hx	333	12.5	7.2	This article
DEMP/HEMA (I-2)	Bz/Hx	333	2.5	10.9	21
DEMP/DEMPC (IV-3)	Bz/Hx	333	3.3	10.6	21
PEO-PI	Bz/Hx	333	28	7.5	13
P-PI	Bz/Hx	333	5.8	10.2	11
DSDA-DDBT	Bz/Hx	333	1.4	10.0	14
I-2	Bz/Cx	323	28	7.0	This article
II-1	Bz/Cx	333	9.0	8.9	This article
II-2	Bz/Cx	333	13.9	7.1	This article
DEMP/HEMA (I-2)	Bz/Cx	333	2.6	11	21
DEMP/DEMPC (IV-3)	Bz/Cx	333	3.1	10.5	21
PEO-PI	Bz/Cx	333	27	5.9	13
P-PI	Bz/Cx	343	6.0	17	11
P-PS/CA(1/1,AC)	Bz/Cx	343	5.8	15.7	11
DSDA-DDBT	Bz/Cx	333	0.35	41	14
I-2	Tol/*n*-Ot	323	5.2	14.3	This article
II-1	Tol/*n*-Ot	333	1.8	18.5	This article
II-2	Tol/*n*-Ot	333	2.7	15.4	This article
DEMP/HEMA (I-2)	Tol/*n*-Ot	333	0.81	19.6	21
DEMP/DEMPC (IV-3)	Tol/*n*-Ot	333	0.91	18.5	21
PEO-PI	Tol/*n*-Ot	353	24	7.5	13
P-PI	Tol/*n*-Ot	353	1.8	18	11
DSDA-DDBT	Tol/*n*-Ot	343	2.1	11.7	14

CONCLUSION

The present VBP-based rubbery polymer membranes displayed a higher specific permeation flux and a lower PV separation factor compared with the DEMP-based membranes. These results occurred because of the VBP-based membranes' larger membrane swelling and higher diffusivity as a result of higher affinity to Bz and lower crosslinking density and of hydrogen bonding having little effect. They displayed rather poor performance of PV to Bz–Hx but good performance to Tol–*n*-Ot. Thus, the PV performance significantly depended on membrane swelling, especially for rubbery polymer membranes.

References

1. Cabasso, I. Ind Eng Chem Prod Res Div 1983, 22, 313.
2. Acharya, H. R.; Stern, S. A.; Liu, Z. Z.; Cabasso, I. J Membr Sci 1988, 37, 205.
3. Garcia Villaluenga, J. P.; Tabe-Mohammadi, A. J Membr Sci 2000, 169, 159.
4. Yamaguchi, T.; Nakao, S.; Kimura, S. Macromolecules 1991, 24, 5522.
5. Yamaguchi, T.; Nakao, S.; Kimura, S. Ind Eng Chem Res 1992, 31, 1914.
6. Enneking, L.; Stephan, W.; Heintz, A. Ber Bunsenges Phys Chem 1993, 97, 912.
7. Sun, F.; Ruckenstein, E. J Membr Sci 1995, 99. 273.
8. Tanihara, N.; Umeo, N.; Kawabata, T.; Tanaka, K.; Kita, H.; Okamoto, K. J Membr Sci 1995, 104, 181.
9. Ho, W. S.; Sartori, G.; Thaler, W. A.; Dalrymple, D. C.; Mastondrea, R. P.; Savage, D. W. ICOM '96, Proceedings, 1996, 1062.
10. Hao, J.; Tanaka, K.; Kita, H.; Okamoto, K. J Membr Sci 1997, 132, 97.
11. Okamoto, K.; Wang, H.; Ijyuin, T.; Fujiwara, S.; Tanaka, K.; Kita, H. J Membr Sci 1999, 157, 97.
12. 12. Wang, H.; Tanaka, K.; Kita, H.; Okamoto, K. J Membr Sci 1999, 154, 221.
13. Wang, H.; Ugomori, T.; Wang, Y.; Tanaka, K.; Kita, H.; Okamoto, K. J Polym Sci, Polym Phys 2000, 38, 1800.
14. Wang, H.; Ugomori, T.; Tanaka, K.; Kita, H.; Okamoto, K.; Suma, Y. J Polym Sci, Polym Phys 2000, 38, 2954.
15. Yamasaki, A.; Shinbo, T.; Mizoguchi, K. J Appl Polym Sci 1997, 64, 1061.
16. Kusakabe, K.; Yongeshiga, S.; Morooka, S. J Membr Sci 1998, 149, 29.
17. Yoshikawa, M.; Tsubouchi, K.; Kitao, T. Sep Sci Technol 1999, 34, 403.
18. Yoshikawa, M.; Tsubouchi, K.; Guiver, M. D.; Robertson, G. P. J Appl Polym Sci 1999, 74, 407.
19. Inui, K.; Noguchi, T.; Miyata, T.; Uragami, T. J Appl Polym Sci 1999, 71, 233.
20. Kai, T.; Tsuru, T.; Nakao, S.; Kimura, S. J Membr Sci 2000, 170, 61.
21. Wang, Y.; Hirakawa, S.; Wang, H.; Tanaka, K.; Kita, H.; Okamoto, K. J Membr Sci, to appear.
22. Yu, Z.; Zhu, W.-X.; Cabasso, I. J Polym Sci, Polym Chem Ed 1990, 28, 227.
23. Crank, J. The Mathematics of Diffusion; Clarendon Press: Oxford, U.K., 1975; pp 238–246.
24. Van Krevelen, D. W. Properties of Polymers; Elsevier: Amsterdam, The Netherlands, 1976; pp. 129–155.
25. Hirchfelder, J. H.; Curtiss, C. F.; Bird, P. B. Molecular Theory of Gases and Liquids; Wiley: New York, 1964; pp 1110–1113.
26. Flory, P. Principles of Polymer Chemistry; Cornell University Press: Ithaca, New York, 1953; Chapter 31.
27. Ponangi, R.; Piintaauro, P. N. J Membr Sci 1998, 144, 25.